MINERALOGIA POLONICA
Vol. 5 — 1974

Bogna DOMINIK *, *Andrzej MANECKI* *,
Krzysztof P. PAWŁOWSKI **

MICROSCOPIC AND X-RAY INVESTIGATIONS OF 2H- AND 3R-GRAPHITE FROM THE MORASKO IRON METEORITE

UKD 549.212.086+548.73:552.61(438.222 Morasko)

Abstract. The presented data were obtained from examinations of graphite separated from coarse-structural octahedrite Morasko. In the meteorite under study this mineral appears in larger concentrations in the form of nodules in paragenesis with troilite, schreibersite, cohenite and kamacite. Cliftonite aggregates, on the other hand, are rare. Graphite from the Morasko meteorite has been found to differ from the Ceylon graphite in a more distinct lamellar structure (the highest L_a/L_c ratio), larger size of crystallites but poorer three-dimensional ordering, and a higher content of rhombohedral structure (3R). The data obtained indicate that this mineral was subject to the activity of destructive forces (shock metamorphism) that caused an increase in the content of rhombohedral structure and a deterioration in three-dimensional ordering. The present authors are of opinion that graphite is an important indicator of the processes of shock and thermal metamorphism that meteorites were submitted to.

INTRODUCTION

Carbon in meteorites may appear as native carbon, carbides, carbonates, hydrocarbons and in solid solution with metallic phases. Native carbon in meteorites is represented by diamond, londsdaleite, graphite and chaoite. In this group graphite is relatively most common. It has been recorded in a variety of meteorites, being most frequent in iron meteorites in which it sometimes appears in larger concentrations in the form of nodules some centimetres in diameter. Such nodules are usually polymineral. Worthy of note are also pseudoregular forms of graphite concentrations, the so-called cliftonite, which was described for the first time by Fletcher (1887).

Graphite appears in the form of two crystallographic varieties, hexagonal and rhombohedral. Graphite crystallites are made up of stacking

* Institute of Mineralogy and Mineral Deposits, Academy of Mining and Metallurgy, Cracow (Kraków, Al. Mickiewicza 30).

** Research and Development Centre of Electro-carbon Factory, Nowy Sącz, P.O. Box 39.

layers that consist of carbon atoms arranged in regular, plane hexagons. Distances between two nearest neighbouring atoms in a layer are 1.42 Å.

The individual layers may be arranged with respect to one another in different ways:

1) in the sequence *ABABAB*... (hexagonal structure), where every other layer in the direction of c axis is translationally identical,
2) in the sequence *ABCABC*... (rhombohedral structure), where every third layer in the direction of c axis is translationally identical.

The individual non-identical layers are always translated with respect to one another by a segment $\frac{a\sqrt{3}}{3}$ in the direction [100].

The hexagonal modification with the space group $P6_3mmc$ is the stable form of the structure. A crystallographic cell has the dimensions $a = 2.456$ Å, $c = 6.708$ Å, and contains four atoms.

In the two varieties of graphite, interlayer distances in crystallites (distances c) vary depending on the degree of spatial ordering in the crystallite from 3.354 Å for ideal graphite to 3.44 Å for non-graphitized carbon structures.

EXPERIMENTAL PROCEDURE

Microscopic examinations. The sample was investigated by optical, electron and scanning microscope. Optical features as well as the forms of graphite concentrations were determined using a microscope for reflected light and examining polished sections of the meteorite. Surface topography and the habit of graphite crystallites were determined by the Tesla 246-B electron microscope. Replica and powder methods were adopted for these investigations. For making replicas triafol matrix technique was applied. The scanning microscope (ISM-S1) proved particularly useful in the investigations of the morphology of graphite.

X-ray examinations. X-ray analyses were performed on the TUR-M-62 X-ray diffractometer with CuK_α radiation, provided with a printing system and a counter. Measurements of the diffraction spectrum were made at a constant counting time and step regulation of the goniometer counter by 0.01—0.03° Θ. The resultant diffraction lines were separated into the components $CuK_{\alpha 1}$ and $CuK_{\alpha 2}$ by Rachinger's method (1948), taking for calculations data from the $CuK_{\alpha 1}$ diffraction lines. Quartz with the grain size about 10 μm was used as standard in size measurements of crystallites and in Fourier analysis. Instumental displacement when measuring interplanar distances was determined from the position of the standard aluminium line. Graphite was heated in Tamman furnace at 1250°C and 1650°C in graphite crucibles in argon atmosphere.

EXPERIMENTAL DATA

Results of microscopic examinations

In the Morasko meteorite graphite forms spherical and oval polymineral concentrations in paragenesis with troilite, sphalerite, schreibersite, cohenite and kamacite (Dominik, in press). In these concentrations it is as a rule a subordinate, rarely a coordinate or dominant, component. Microscopic analyses in reflected light revealed optical features typical for this mineral, i.e. strong bireflectance and anisotropy.

In the most common type of nodules graphite concentrates only in the marginal parts, assuming crescent- or "*l*"-shaped forms (the so-called crescent graphite according to El Goresy (1965)). In these concentrations graphite forms a variety of fan-shaped (Phot. 12), feathery, sperulitic--concentric (Phot. 3) or random (Phot. 4) aggregats. In the nodules in question there are numerous graphite inclusions in troilite concentrated in the marginal parts (Phot. 5); they are missing, on the other hand, in troilite of the central parts.

In another type of nodules, equally common as those described, graphite appears in the troilite core of these polymineral concentrations. The internal rim of such nodules is formed by schreibersite, the external one — by fractured and graphitized cohenite. Similar fractures have been also observed in troilite. In the troilite core of these nodules, graphite is a subordinate component. Very rare are nodules that have a troilite-graphite core, the two minerals appearing in equal quantities. The core is coated with graphite, whitelockite, cliftonite with graphite and external, schreibersite, rims. In troilite graphite concentrates as scales forming in places feathery and palm aggregates, or in the form of wormy aggregates, the latter being similar to retort graphite. Nodules with the core made up of graphite are found only sporadically. In their centre palm aggregates of graphite scales may be observed whereas in the marginal parts there are spherulitic and fan-shaped concentrations.

Besides the graphite concentrations discussed, cliftonite has been ascertained in the Morasko meteorite (Phot. 6). It appears as isolated single forms or aggregates in kamacite or else it forms cliftonite and cliftonite-graphite rims around the polymineral nodules. It should be mentioned that cliftonite never occurs in the central parts of nodules.

Investigations performed by electron and scanning microscope were to afford information on the habit and surface topography of graphite of cosmic origin. When making matrices, extraction of small graphite aggregates from the polished surface of the meteorite was usually noted. Such concentrations of graphite lamellae are shown in Photograph 7. In powder preparations the presence of graphite lamellae with the characteristic hexagonal habit has been ascertained (Phot. 8). Much better data are obtained from scanning microscope. In nodules with graphite, idiomorphic blocks of crystallites of the size 1—3 μm predominate (Phot. 9), while large flat graphite lamellae with hexagonal habit are rare and are not more than 80 μm broad and 2—3 μm thick (Phot. 10).

Results of X-ray examinations

For X-ray examinations graphite was separated from the central parts of larger nodules, i.e. without cliftonite. Upon separation the samples were handled so as to avoid any comminution or grinding that could have disturbed the structure of graphite.

Measurement of interplanar distances. Interplanar distances d_{002} were determined from the position of lines 002, 004, 006, 008. The position of

the interference peak maximum was assumed to be the position of the lines.

The values d_{002} obtained from the measurements of the position of the successive lines 001 were extrapolated by the function $f(\Theta) = \frac{1}{2}\left(\frac{\cos^2\Theta}{\sin\Theta} + \frac{\cos^2\Theta}{\Theta}\right)$ to the value $\Theta = \frac{\pi}{2}$. The value obtained from extrapolation was assumed to be interplanar distance.

Probability p that two neighbouring planes are not ordered was determined from Bacon's formula (1951)

$$d_{002} = 3.440 - 0.086\,(1 - p) - 0.064\,p\,(1 - p)$$

Mean square displacement of neighbouring parallel planes (Δ_{12}^2) was calculated from Ruland's formula (1965)

$$d_{002} = 3.354 + 0.4247\,\Delta_{12}^2$$

Size measurement of crystallites from half-breadth of lines. The size of crystallites was calculated from half-breadth of lines 004, 110, 112 basing on Scherrer's formula:

$$L_{hkl} = \frac{k \cdot \lambda}{\Delta B_{hkl} \cdot \cos\Theta_{hkl}}$$

where:

L_{hkl} — crystallite size in the direction perpendicular to the reflecting plane hkl

λ — wave length of $CuK_{\alpha 1}$ radiation

Θ_{hkl} — maximum position of $K_{\alpha 1}$ line

ΔB_{hkl} — $\sqrt{(B^G_{hkl})^2 - (B^w)^2}$, where:

B^G — half-breadth of the respective graphite line $K_{\alpha 1}$

B^w — half-breadth of the $K_{\alpha 1}$ line of quartz standard extrapolated to Θ_{hkl}.

Constant k (for calculating the diameter of crystallites) was given by Hirai's formula (1969).

$$k = 0.90 + (1.84 - 0.90)\,p$$

For the height of crystallites ($\perp$ 001) k does not depend on the degree of graphitization of the sample and is 0.94.

Fourier analysis of the shape of diffraction lines. Fourier analysis was applied to $K_{\alpha 1}$ components of the lines 002, 004 and 110, with the coefficients A_n of the pure graphite line distribution determined by means of Lipson-Beevers bands and the effect of instrumental broadening eliminated. The coefficients A_n were computed from the formula (Warren 1959)

$$A_n = \frac{H_r(n)G_r(n) + H_i(n)G_i(n)}{G_r^2(n) + G_i^2(n)}$$

where:

$H_r(n)$ and $H_i(n)$ are the transforms characterizing the experimental peak and are given by the formulae:

$$H_r(n) = \frac{1}{a}\sum_{-a/2}^{a/2} h(x)\cos 2\pi x\left(\frac{n}{a}\right)$$

$$H_i(n) = \frac{1}{a}\sum_{-a/2}^{a/2} h(x)\sin 2\pi x\left(\frac{n}{a}\right)$$

and $G_r(n)$ and $G_i(n)$ are the analogous quantities characterizing instrumental broadening (from the respective peak of the quartz standard).

Fourier analysis was carried out with the division of lines into $a = 48$.

The mean number of N_3 layers in crystallites was evaluated from the plots of A_n *vs*·n as the point of intersection of the tangent at $n = 0$ with n axis.

Distribution coefficients of the line 110 may be presented as:

$$A_n(hkl) = \langle exp\,[2\pi i\,(X_n h + Y_n k)]\,\rangle = P_n^o + (P_n^+ + P_n^-)\cos 2\pi\left(\frac{2}{3}h + \frac{1}{3}k\right)$$

where:

P_n^o — probability of zero displacements

P_n^+, P_n^- — probability of displacements $X_n = \pm\frac{2}{3}$

$$Y_n = \pm\frac{1}{3}$$

i.e. $A_1(110) = P_1^+ + P_1^-$ is the probability that two neighbouring layers are in the ordering of graphite, $A_2(110) = P_2 + (P_2^+ + P_2^-)$ is the probability that there are the sequence *ABABABA*... (P_2^o — hexagonal structure) and the sequence *ABCABCAB*.. ($P_2^+ + P_2$) — rhombohedral structure).

Estimation of the content of rhombohedral structure in the sample. To evaluate the content of rhombohedral structure, the total intensity of the strongest rhombohedral reflection $10\bar{1}\,\frac{2}{3}$ and the accompanying hexagonal reflection $10\bar{1}1$ was measured. Accordingly, thorough examinations of the diffraction spectrum in the angle range 20°30′ — 22°30′ were made and then the individual lines were graphically separated. The ratio of intensity of the line $10\bar{1}\,\frac{2}{3}$ to the sum of intensities of the lines $10\bar{1}\,\frac{2}{3}$ and $10\bar{1}1$ related to the content of the structures *ABABA*... and *ABCABCABC*..., calculated from Fourier analysis of the line 110, was assumed to be the percentage of the content of rhombohedral structure.

In the case of meteorite graphite, a larger error of measurement was involved since it is difficult to separate lines of impurities interfered with those of graphite.

Calculations of structural parameters of meteorite graphite were made and the results compared with the data obtained for natural Ceylon graphite in raw state and heated four times for 1 hour at 2800°C. The results are listed in Tables 1, 2 and 3. The data (Tab. 1) on the percentage

of disordered layers and the mean square displacement of layers indicate that within the crystallites of meteorite graphite the layers show a lower degree of spatial ordering. Higher d_{002} value and greater values of parameters p, Δ_{12}^2 imply a poorer graphitization of the meteorite graphite. The

Table 1

Interplanar spacings

	Extrapolated d_{002}	Amount of disordered layers %	Δ_{12}^2
Morasko graphite	3.3608	23.0	0.016
Ceylon graphite	3.3590	16.5	0.012
Ceylon graphite heated four times	3.3585	15.2	0.010

results of size measurements of crystallites are given in Table 2. It is characteristic that the height of crystallites, calculated both from half-breadth and Fourier analysis, is the greatest (just as the diameter) for the meteorite graphite. The diagonal dimension I_{112} (indicating the degree of spatial ordering) is, on the other hand, the smallest for the meteorite graphite and the largest for the Ceylon graphite fourfold graphitized. This is in accordance with the data presented in Table 2. Data from Fourier analysis of the line 110 and the content of rhombohedral structure in the samples are given in Table 3. All the three samples have an approximate value of probability that two neighbouring layers are mutually

Table 2

Size of crystallites in (Å)

	From half-breadth of lines			From Fourier analysis	
	Diameter of crystallite (Å)	Diagonal dimension L_{112} (Å)	Height of crystallite (Å)	Amount of parallel layers $N3$	Height of crystallite (Å)
Morasko graphite	700	290	410	112	377
Ceylon graphite	450	315	320	92	309
Ceylon graphite heated four times	530	370	340	99	333

ordered (about 96%). There is also an insignificant difference in the content of layers arranged in graphite sequences *ABAB*... (hexagonal) and *ABCABC*... (rhombohedral). The total graphite content *ABAB*... and *ABCABC*... attain for all the samples the value of 88—90%, which means

Table 3

Amount of rhombohedral structure

	% of layers being in the ordering of graphite with respect to the nearest neighbouring	% of layers packed in the sequence *ABAB*... and *ABCABC*...	Amount of rhombohedral structure in %
Morasko graphite	96.7	90	16—20
Ceylon graphite	96.4	89	13.9
Ceylon graphite heated four times	96.0	88	8.0

that in the samples under study (also in the meteorite graphite) the content of free carbon in single and double layers does not exceed about 10% of the total mass of carbon.

The meteorite graphite is characterized by a higher content of rhombohedral structure when compared with natural graphites (from 16—20% in meteorite graphite, 13% in natural Ceylon graphite in raw state, 8% in heated graphite). The sample of meteorite graphite was heated at 1250°C and 1650°C. In consequence, the content of rhombohedral structure was found to have decreased in both cases down to about 11%.

CONCLUSIONS

Graphite filling the nodules in the Morasko octahedrite visibly differs from the Ceylon graphite in:

a. The shape of crystallites — a more distinct lamellar structure (the highest L_a/L_c ratio),

b. Larger size of crystallites but lower degree of three-dimensional ordering of the layers,

c. A higher content of rhombohedral structure,

d. The presence of cliftonite.

The data obtained indicate that the meteorite graphite was subject to the activity of destructive forces (shock metamorphism) that caused an increase in the content of rhombohedral structure and a deterioration in

three-dimensional ordering. These processes however were not accompanied by high temperatures (higher than about 1250°C) as this would have resulted in a decrease in the content of rhombohedral graphite. Great susceptibility of graphite to structural changes under the influence of pressure and high temperature makes this mineral an important indicator of the processes of shock and thermal metamorphism in meteorites.

REFERENCES

BACON G. E., 1951: Interlayer spacings in graphite. *Acta cryst.* 4, 558.

DOMINIK B., 1976; Mineralogical and chemical study of coarse octahedrite Morasko (Poland). *Prace mineralogiczne, 47* (in press).

FLETCHER L., 1887: On a meteoritic iron found in 1884 in the subdistrict of Youndegin, Western Australia, and containing cliftonite, a cubic form of graphitic carbon. *Min. Mag.* 7, 34, 121.

EL GORESY A., 1965: Mineralbestand und Strukturen der Graphit und Sulfideinschlüsse in Eisenmeteoriten. *Geoch. Cosm. Acta* 29, 10, 1131.

RACHINGER W. A., 1948: The resolution of X-ray doublet diffraction lines into components. *J. Sci. Instr.* 25, 254.

RULAND W., 1965: X-ray studies on the structure of graphite carbons. *Acta cryst.* 18, 992.

WARREN B., 1959: X-ray studies of deformed metals. *Prog. in Metal Phys.* 8, 147.

Bogna DOMINIK, Andrzej MANECKI,
Krzysztof P. PAWŁOWSKI

MIKROSKOPOWE I RENTGENOGRAFICZNE BADANIA GRAFITU 2H I 3R Z METEORYTU ŻELAZNEGO MORASKO

Streszczenie

Przedstawione wyniki badań dotyczą grafitu wyseparowanego z grubostrukturalnego oktaedrytu Morasko. Do badań zastosowano metody mikroskopowe (mikroskopy: optyczny, elektronowy i skaningowy) oraz rentgenograficzne. Grafit tworzy zwykle większe koncentracje w formie nodul w paragenezie z troilitem, schreibersytem, cohenitem i kamacytem. Rzadkie są agregaty cliftonitu. Porównano wyniki badań rentgenostrukturalnych grafitu meteorytowego z grafitem ziemskim z Cejlonu. Stwierdzono, że grafit z meteorytu Morasko różni się od grafitu cejlońskiego: wyraźniejszą budową płytkową (najwyższy stosunek L_a/L_c), większymi wymiarami krystalitów przy mniej dokładnym uporządkowaniu trójwymiarowym, większym udziałem struktury romboedrycznej i obecnością odmiany pseudoregularnej — cliftonitu. Uzyskane wyniki wskazują, że minerał ten poddany był działaniu sił niszczących (metamorfizm uderzeniowy), które spowodowały wzrost udziału struktury romboedrycznej i zmniejszenie uporządkowania trójwymiarowego. Siły niszczące działały w stosunkowo niskich temperaturach, na co wskazują wyniki badań rentgenostrukturalnych próbek wyżarzonych w temperaturze 1250°C i 1650°C (w obu przypadkach stwierdzono obniżenie zawartości struktury romboedrycznej). Zdaniem autorów grafit jest ważnym wskaźnikiem procesów metamorfizmu uderzeniowego i termicznego, jakim podlegały meteoryty.

Богна ДОМИНИК, Анджей МАНЕЦКИ,
Кшиштоф П. ПАВЛОВСКИ

МИКРОСКОПИЧЕСКИЕ И РЕНТГЕНОВСКИЕ ИССЛЕДОВАНИЯ ГРАФИТА 2H И 3R ИЗ ЖЕЛЕЗНОГО МЕТЕОРИТА МОРАСКО

Резюме

Представлены результаты исследования графита, извлеченного из крупноструктурного метеорита Мораско. Применялись микроскопические наблюдения (оптический, электронный и сканинг-микроскоп) и рентгенографические анализы. Графит представлен, как правило, в виде нодулей в парагенезисе со шрейберзитом, когенитом и камацитом. Редко встречаются агрегаты клифтонита. Рентгеноструктурное сравнение метеоритного графита с земным графитом из Цейлона показали, что метеоритный графит отличается более четкой плитчатой структурой (самый высокий показатель L_a/L_c), более крупными размерами кристаллитов с меньшей упорядоченностью в трехмерном пространстве, большим участием ромбоэдрической структуры и присутствием псевдорегулярной разновидности — клифтонита. На основании полученных данных можно предполагать, что этот минерал подвергался действию разрушительной силы (ударный метаморфизм), которая обусловила увеличение содержания ромбоэдрической структуры и уменьшение трехмерного упорядочения. Разрушительная сила действовала при сравнительно низкой температуре, как показывают данные рентгеноструктурного анализа образцов, прокаленных при 1250° и 1650°C (в обу случаях наблюдалось уменьшение содержания ромбоэдрической структуры). По мнению авторов, графит является важным показателем процессов ударного и термического метаморфизма, которым подвергаются метеориты.

PLATE I (PLANSZA I, ТАБЛИЦА I)

Phot. 1. Graphite concentration made up of fan-shaped aggregates. 1 nicol, × 200
Skupienie grafitu zbudowane z agregatów wachlarzowatych. Nik. 1. pow. 200 ×
Скопления графита, сложенные веерообразными агрегатами. Ник. 1, увел. 200 ×

Phot. 2. Concentration as above. Crossed nicols, × 200
Skupienie j. w. Nik. +, pow. 200 ×
Скопление к. в. Ник. +, увел. 200 ×

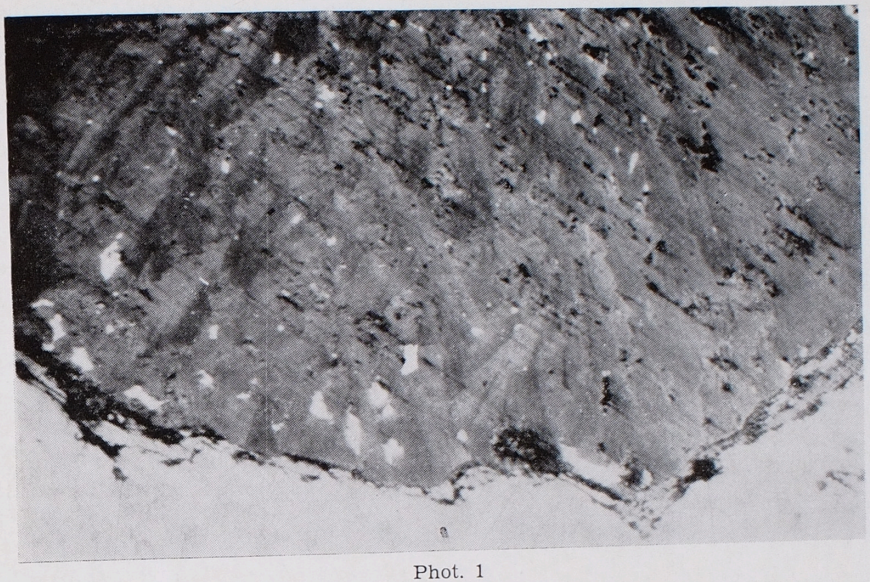

Phot. 1

Phot. 2

Bogna DOMINIK, Andrzej MANECKI, Krzysztof P. PAWŁOWSKI — Microscopic and X-ray investigations of 2H- and 3R-graphite from the Morasko iron meteorite

PLATE II (PLANSZA II, ТАБЛИЦА II)

Phot. 3. Spherulitic-radial graphite aggregates. Crossed nicols, × 200
Agregaty grafitu o budowie sferolitowo-radialnej. Nik. +, pow. 200 ×
Агрегаты графита со сферолито-радиальным строением. Ник. +, увел. 200 ×

Phot. 4. Graphite aggregate with random structure. Crossed nicols, × 200
Agregat grafitu o budowie bezładnej. Nik. +, pow. 200 ×
Агрегат графита с беспорядочным строением. Ник. +, увел. 200 ×

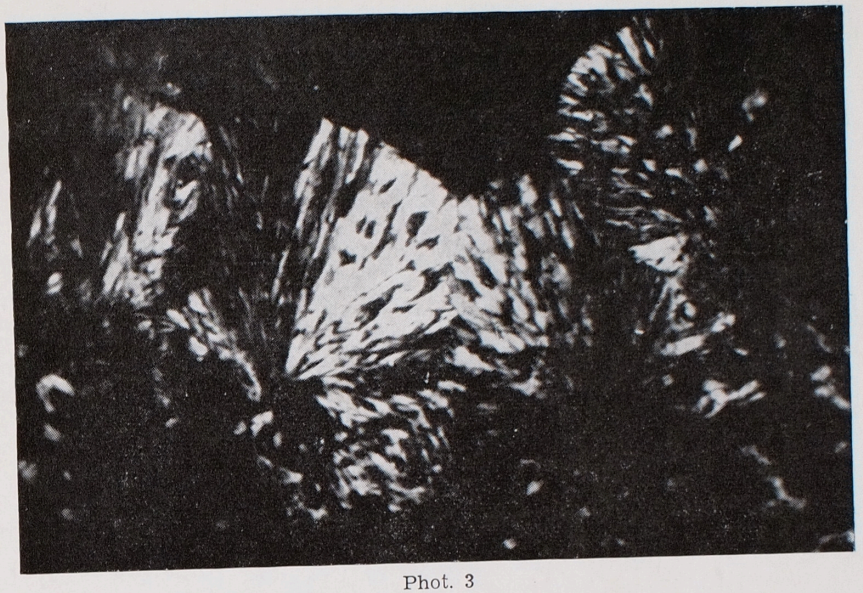

Phot. 3

Phot. 4

PLATE III (PLANSZA III, ТАБЛИЦА III)

Phot. 5. Graphite intergrowths in the marginal part of a troilite nodule. Crossed nicols, × 80
Przerosty grafitu w brzeżnej części noduli troilitowej. Nik. +, pow. 80 ×
Включения графита в краевой части троилитового нодуля. Ник. +, увел. 80 ×

Phot. 6. Single cliftonite form. 1/2 crossed nicols, × 300, immersion
Pojedyncza forma cliftonitu. Nik. 1/2+, pow. 300 × w imersji
Отдельная форма слифтонита. Ник. 1/2 +, увел. 300 ×, иммерсия

Phot. 5

Phot. 6

Bogna DOMINIK, Andrzej MANECKI, Krzysztof P. PAWŁOWSKI — Microscopic and X-ray investigations of 2H- and 3R-graphite from the Morasko iron meteorite

PLATE IV (PLANSZA IV, ТАБЛИЦА IV)

Phot. 7. Electron image — concentration of graphite lamellae. × 7400
Obraz elektronowy — skupienie płytek grafitowych, pow. 7400 ×
Электронный образ — скопление графитовых пластинок. Увел. 7400 ×

Phot. 8. Electron image — hexagonal graphite lamella. × 13 100
Obraz elektronowy — płytka grafitu o formie heksagonalnej, pow. 13 100 ×
Электронный образ — пластинка графита гексагональной формы. Увел. 13 100 ×

Phot. 9. Scanning electron image — idiomorphic blocks of graphite crystallites. × 1500
Obraz elektronowy skaningowy — idiomorficzne bloki krystalitów grafitu, pow. 1500 ×
Сканинг-электронный образ — идиоморфные блоки кристаллитов графита. Увел. 1500 ×

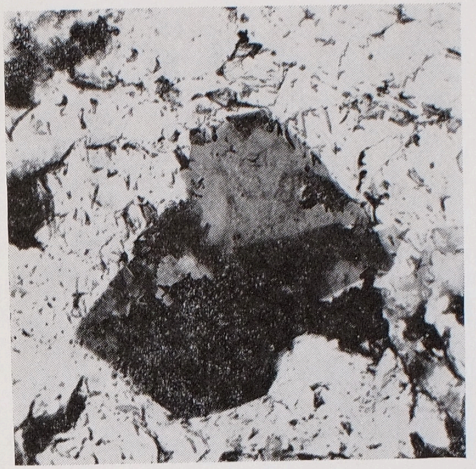

Phot. 7

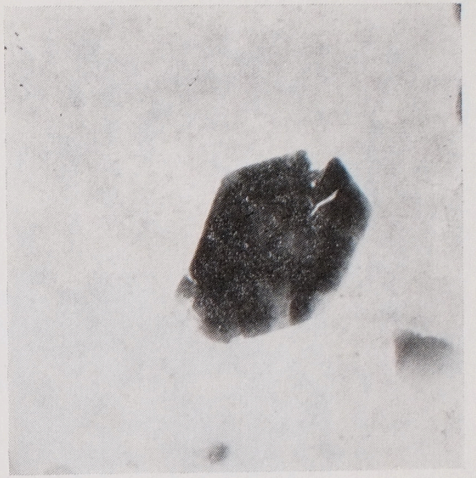

Phot. 8

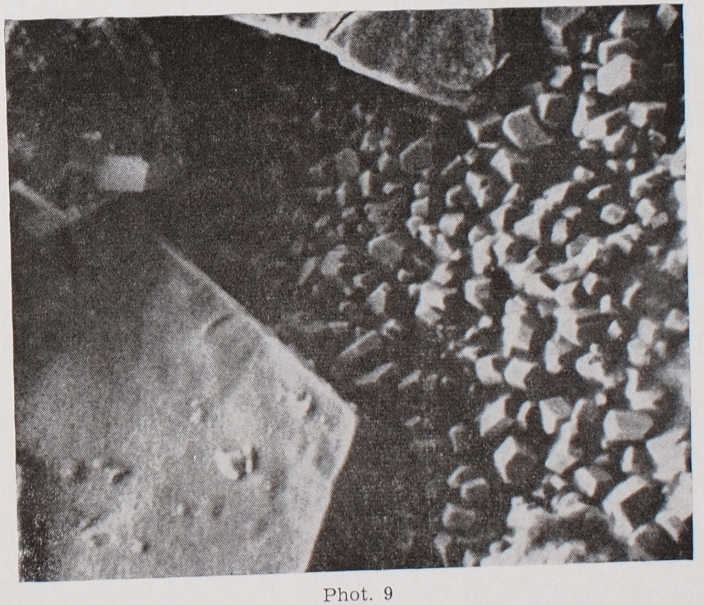

Phot. 9

Bogna DOMINIK, Andrzej MANECKI, Krzysztof P. PAWŁOWSKI — Microscopic and X-ray investigations of 2H- and 3R-graphite from the Morasko iron meteorite

PLATE V (PLANSZA V, ТАБЛИЦА V)

Phot. 10. Scanning electron image — large hexagonal graphite lamellae. × 650
Obraz elektronowy skaningowy — duże heksagonalne płytki grafitu, pow. 650 ×
Сканинг-электронный образ — крупные гексагональные пластинки графита. Увел. 650 ×

Phot. 10